On the dynamics of a single-bit stochastic-resonance memory device

S.A. Ibáñez[1], P.I. Fierens[1,3,a], R.P.J. Perazzo[1], G.A. Patterson[2], and D.F. Grosz[1,2,3]

[1] Instituto Tecnológico de Buenos Aires, Av. Eduardo Madero 399, Buenos Aires (C1106ACD), Argentina
[2] Departamento de Física, FCEN, Universidad de Buenos Aires, Intendente Güiraldes 2160, Buenos Aires (C1428EGA), Argentina
[3] Consejo Nacional de Investigaciones Científicas y Técnicas, Av. Rivadavia 1917, Buenos Aires (C1033AAJ), Argentina

Abstract. The increasing capacity of modern computers, driven by Moore's Law, is accompanied by smaller noise margins and higher error rates. In this paper we propose a memory device, consisting of a ring of two identical overdamped bistable forward-coupled oscillators, which may serve as a building block in a larger scale solution to this problem. We show that such a system is capable of storing a single bit and its performance improves with the addition of noise. The proposed device can be regarded as asynchronous, in the sense that stored information can be retrieved at any time and, after a certain synchronization time, the probability of erroneous retrieval does not depend on which oscillator is being interrogated. We characterize memory persistence time and show it to be maximized for the same noise range that both minimizes the probability of error and ensures synchronization. We also present experimental results for a hard-wired version of the proposed memory, consisting of a loop of two Schmitt triggers. We show that this device is capable of storing a single bit and does so more efficiently in the presence of noise.

1 Introduction

The increasing capacity of modern computers has been driven by Moore's Law, which postulates that the number of transistors in an integrated circuit doubles roughly every two years. However, as noted in reference [1], noise immunity and power consumption do not follow Moore's law. On the contrary, higher transistor density and power consumption require the use of smaller supply voltages. All these factors together lead to smaller noise margins and higher error rates in computation [2,3]. There have been several proposals to solve this problem, e.g., references [1,4,5] take explicitly into account the fact that the results of a computation may be correct only with some probability, and reference [6] uses a set of orthogonal noise processes to represent logic values. Recently, it was shown how to implement basic logical operations (OR, AND, NOR, NAND) using nonlinear systems such that their performance improves in the presence of noise [7–9], a signature of stochastic resonance.

Stochastic resonance (SR) is usually associated with a nonlinear system where the noise helps, an otherwise weak signal, to induce transitions between stable equilibrium states [10–12]. The phenomenon of stochastic resonance has been studied in a large number of applications, ranging from biological and neurological systems [13–15] to information transmission sustained by noise [16–23] and information storage [24–26]. In references [24,25] a ring of identical oscillators was shown to be able to sustain a travelling wave with the aid of noise, long after the harmonic driving signal had been switched off. It is only natural to ask whether such a scheme can be used to store data, i.e., aperiodic signals, in noisy environments. We show that such a ring of two bistable oscillators is capable of storing a single bit of information via stochastic resonance. Memory performance is characterized in terms of the probability of an erroneous bit detection. In particular, we show that by the addition of a small amount of noise, the system outperforms the deterministic (noiseless) case. We also show that information can be retrieved from any of the two oscillators, obtaining the same probability of error after an elapsed 'synchronization' time that decreases with increasing noise. Moreover, there is a noise range that yields a minimum probability of error with a nearly minimum synchronization time. By comparing system performance to that of the noiseless case, we define a memory persistence time and show it to exhibit a stochastic-resonance behavior.

Finally, we build a model of the proposed system with two Schmitt triggers (STs) in a loop configuration. STs provide a convenient 'discrete' model of the bistable oscillators [27,28]. By feeding each ST with Gaussian noise, we show that the system is capable of storing a single bit, and it does so more efficiently for an optimum amount of noise.

[a] e-mail: pfierens@itba.edu.ar

The paper is organized as follows: Section 2 describes the system under analysis. In Section 3 we present simulation results and characterize the performance of the proposed memory device. Experimental results corresponding to a loop of Schmitt triggers are presented in Section 4. Concluding remarks are found in Section 5.

2 The system: a ring of two oscillators

The system consists of a ring of bistable forward-coupled oscillators. The coupling is proportional to the amplitude of each oscillator, as it is described in reference [24]. The system with N oscillators is described by the following stochastic differential equations

$$dx_n = \left[-\frac{\partial U_1}{\partial x}(x_n) + \epsilon \frac{x_{n-1}}{x_0} \right] dt + \sigma dW_n \qquad (1)$$

for $1 < n \leq N$, and

$$dx_1 = \left[-\frac{\partial U_1}{\partial x}(x_1) + \epsilon \frac{x_N}{x_0} \right] dt + \sigma dW_1 \qquad (2)$$

for the first oscillator, where W_i represents standard Brownian motion, spatially uncorrelated ($\langle W_i \rangle = 0$, and the correlation $\langle dW_i\, dW_j \rangle = \delta_{ij} dt$), σ^2 is the noise intensity, ϵ is the coupling strength between adjacent oscillators, and $U_1(x)$ is the one-dimensional potential defined by

$$U_1(x) = U_0 \left(\frac{x}{x_0} \right)^2 \left[\left(\frac{x}{x_0} \right)^2 - 2 \right]. \qquad (3)$$

We are interested in the shortest ring capable of storing information. We shall show that a loop of only two forward-coupled bistable oscillators not only presents an interesting dynamic behavior, but it can also work as a one-bit memory device. In the case of a ring comprising two oscillators, equations (1)–(2) can be written as

$$d\boldsymbol{x} = -\nabla U_2(\boldsymbol{x})\, dt + \sigma d\overrightarrow{W}, \qquad (4)$$

where $d\overrightarrow{W} = (dW_1, dW_2)$ is the noise vector and the bidimensional potential, $U_2(x_1, x_2)$, is expressed as

$$U_2(x_1, x_2) = U_1(x_1) + U_1(x_2) - \epsilon \frac{x_1 x_2}{x_0}. \qquad (5)$$

This system is similar to that in reference [29] and, interestingly, it also resembles that of two Josephson junctions symmetrically inserted into a superconducting loop [30,31]. It is simple to show that equations (1)–(2) cannot be written in the form of equation (4) for $N > 2$. It is useful to interpret equation (4) as the equation of motion of a particle in the bidimensional potential in equation (5).

In the absence of noise, and depending on the coupling strength, the system exhibits three different behaviors, and hence two bifurcations between them; the first bifurcation at $\epsilon = 2U_0/x_0$, and the second at $\epsilon = 4U_0/x_0$. When $\epsilon < 2U_0/x_0$, the potential in equation (5) presents one unstable equilibrium (i.e. a local maximum) at the origin $x_1^M = x_2^M = 0$. It also exhibits four stable equilibrium points, one on each quadrant in the x_1-x_2 phase space (see Fig. 1). While the equilibrium points located in the upper-right and lower-left quadrants are global minima, the equilibria located in the other two quadrants correspond to local minima. As the coupling strength ϵ increases, the wells corresponding to the global minima become deeper, and the wells of the local minima become shallower.

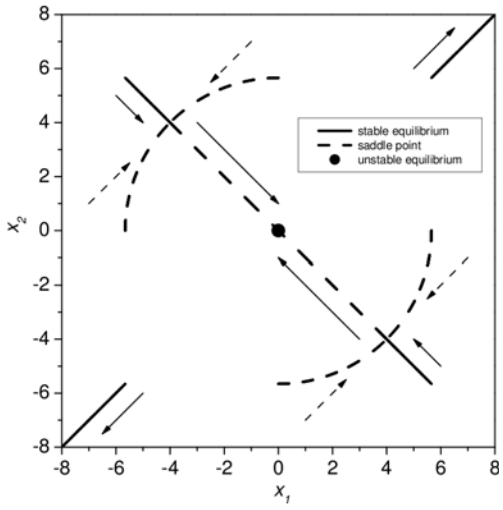

Fig. 1. Phase-space diagram showing the system critical points. Full lines correspond to stable equilibrium points and dashed lines correspond to saddle points. The arrows indicate the direction of increasing of ϵ.

For $\epsilon = 2U_0/x_0$ the system undergoes a pitchfork bifurcation, where the local minima become saddle points, the equilibrium points located in the upper-right and lower-left quadrants remain global minima, and the origin remains a local maximum, as can be seen in Figure 1. There is another pitchfork bifurcation at $\epsilon = 4U_0/x_0$. In this case, the unstable equilibrium point $x_{1,M} = x_{2,M} = 0$ develops into a saddle point. In this situation, the system is notably similar to the one-particle bistable potential in Kramer [32].

In this work, we focus solely on the region $0 < \epsilon < 2U_0/x_0$ where the most interesting behavior is found. In Figure 2, we show the bidimensional potential in equation (5) for the particular case of $\epsilon \approx 0.56\, U_0/x_0$.

2.1 Four-state model

It is customary to approximate the behavior of a particle in a bistable potential by a two-state model (see, e.g., [11,12]). Similarly, we can approximately describe the behavior of the system in equation (4) as that of a system with four discrete states, one for each equilibrium point of the potential in equation (5). Let us enumerate the states as 0 through 3, starting from the equilibrium point in the upper-right quadrant of Figure 1 and moving

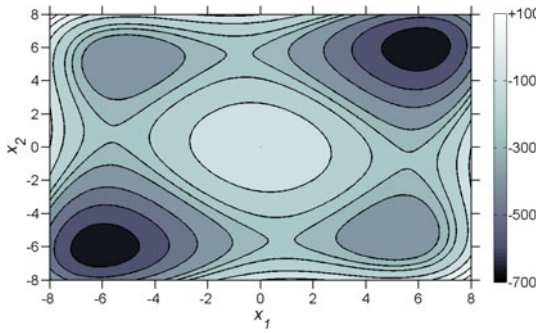

Fig. 2. (Color online) The potential in equation (5) for $U_0 = 256$, $x_0 = \sqrt{32}$ and $\epsilon = 25$.

in counter-clockwise direction. If we denote by $n_i(t)$ the probability of finding the particle in the state i at time t, then the behavior of the system can be described by the following equation

$$\dot{\boldsymbol{n}} = \mathbb{W} \cdot \boldsymbol{n}, \tag{6}$$

where $\boldsymbol{n} = (n_0, n_1, n_2, n_3)^T$ and $\mathbb{W}$ is the transition matrix. We can estimate these transition rates as (see, e.g., [32,33]) $W_{ij} \approx K_{ij} \exp\ -2\Delta U_{ij}/\sigma^2$, where K_{ij} is a constant and ΔU_{ij} is the potential barrier that the particle has to overcome when moving from state i to state j. Symmetries present in the potential in equation (5) (see Fig. 2) allow us to reduce the problem to the calculation of four transition rates dependent on the following potential barriers

$$\Delta U_{ij} = |j-i| U_0 \left(1 + (-1)^i \frac{\epsilon x_0}{2|j-i|U_0}\right)^2 \tag{7}$$

for $ij = 01,\ 10,\ 13,\ 02$. We shall come back to the four-state model in Section 3.1.

3 Simulation results

In order to store one bit, we drive the first oscillator with a short pulse of amplitude P_0 and duration T_P. Since we are interested in a storage system that works solely in the presence of noise, we consider pulse intensities which are too low to force the system out of the deeper equilibrium states. In particular, for our simulations we set P_0 such that the work exerted by the driving force is smaller than the potential barrier ΔU_{01} in equation (7).

Memory retrieval from oscillator i, at interrogation time t_0, is performed by taking the average

$$\bar{x}_i(t_0) = \frac{1}{T_P} \int_{t_0}^{t_0+T_P} x_i(t) dt, \tag{8}$$

and comparing $\bar{x}_i(t_0)$ to a fixed threshold, arbitrarily set to 0. The system incurs in an error when $\bar{x}_i(t_0) < 0$.

We assess memory performance by observing the time evolution of the probability of error upon retrieval of the stored bit. We shall call $p_{e,i}$ the probability of error on retrieval from the i-th oscillator and use p_e as a shorthand

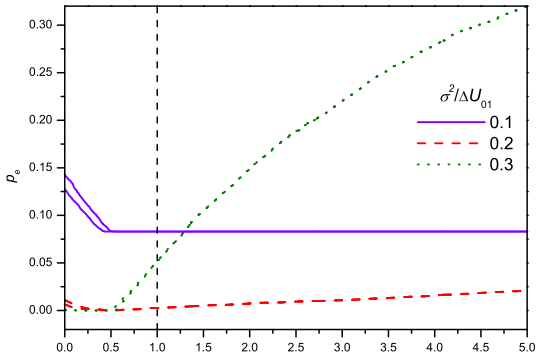

(a) p_e vs. time for $\epsilon = 75$

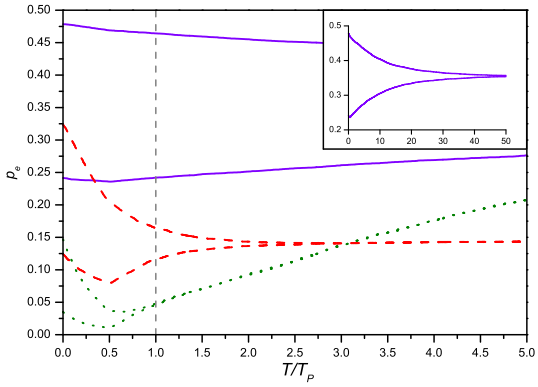

(b) p_e vs. time for $\epsilon = 25$

Fig. 3. (Color online) The evolution of the probability of error as a function of noise intensity and coupling strength. In both figures, $p_{e,1}$ is always smaller than $p_{e,2}$.

for 'probability of error'. We estimate p_e as the number of errors divided by the total number of realizations

$$p_{e,i} = \frac{\#\text{ number of errors in oscillator } i}{\#\text{ total number of realizations}}, \text{ for } i = 1, 2. \tag{9}$$

The results in this section correspond to a system with $U_0 = 256$ and $x_0 = \sqrt{32}$. The pulse duration was set to $T_P = 5$ and the pulse amplitude to $P_0 = 0.13\Delta U_{01}/x_{eq}$, where $x_{eq} = x_0\sqrt{1 + \epsilon x_0/4U_0}$ is the distance from the global minima to the coordinate axes. For each noise level, we performed 10000 numerical simulations of equation (4), with initial conditions chosen randomly in the rectangular region $[-9.0 : 9.0] \times [-9.0 : 9.0]$, using the Euler-Maruyama method [34] with an integration step $\Delta t \sim 10^{-4} T_P$.

In Figure 3 we show the evolution of the probability of error as a function of noise intensity and coupling strength. The vertical dashed line indicates the instant at which the drive is turned off. Observe that the probability of error for the first oscillator is always smaller than that for the second. In the case of strong coupling (Fig. 3a), the probability of error improves with time in both oscillators while the driving pulse is on. For a small noise intensity, the degradation of the error probability is almost negligible after turning off the pulse, since noise is not strong enough to overcome the potential barrier. On the other

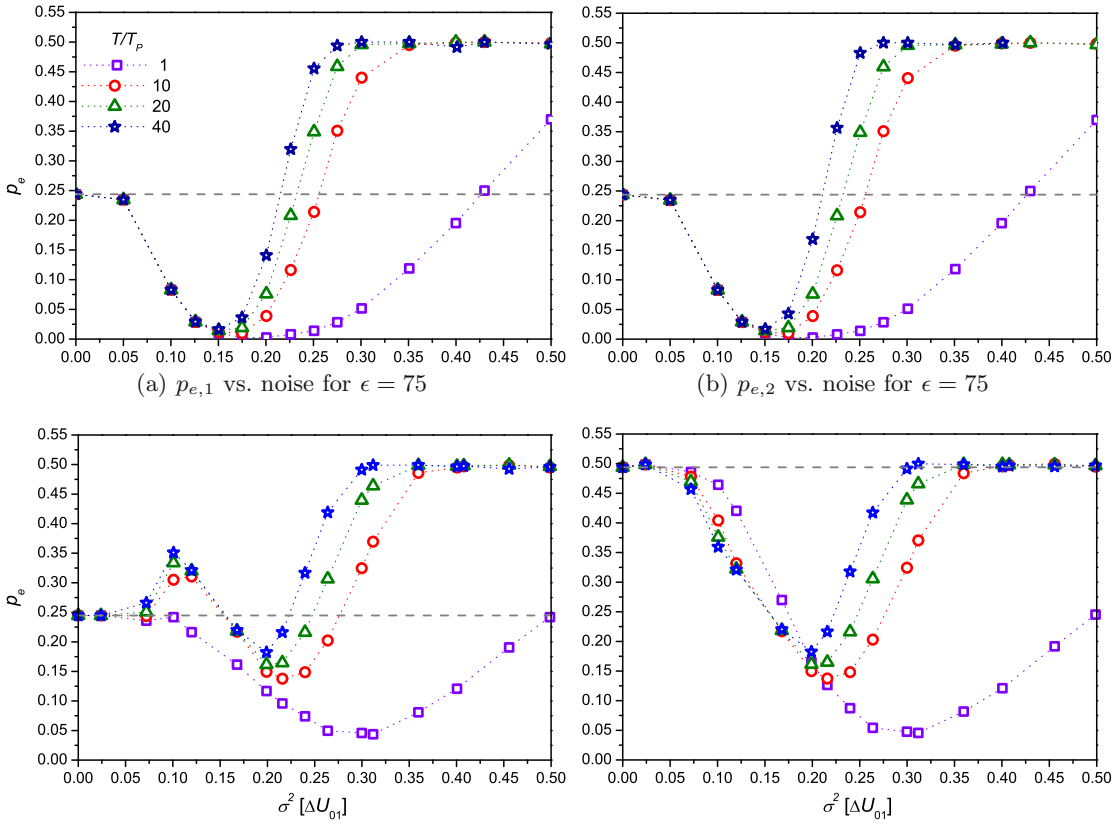

(a) $p_{e,1}$ vs. noise for $\epsilon = 75$ (b) $p_{e,2}$ vs. noise for $\epsilon = 75$

(c) $p_{e,1}$ vs. noise for $\epsilon = 25$ (d) $p_{e,2}$ vs. noise for $\epsilon = 25$

Fig. 4. (Color online) Probability of error as function of noise intensity for different observation times ($T = T_P$, $10T_P$, $20T_P$, $40T_P$) and coupling strengths ($\epsilon = 25, 75$).

hand, performance degrades at a faster pace for higher noise intensities. While the behavior of both oscillators is very similar for a strong coupling, for a weaker coupling and a small noise intensity, the first oscillator outperforms the second (see Fig. 3b). Indeed, the first oscillator rapidly follows the driving pulse, which is stronger than the weakly-coupled output of the second oscillator. However, the second oscillator is driven by the sub-threshold output of the first oscillator and, thus is not able to immediately follow the external drive. When the driving pulse is turned off $p_{e,1}$ slowly increases because of noise and the influence of the second oscillator. On increasing the noise intensity, the performance of both oscillators becomes similar independently of the coupling strength.

Figure 4 shows the estimated probability of error for each oscillator as a function of noise intensity and for increasing times ($T_1 = T_P$, $T_2 = 10\,T_P$, $T_3 = 20\,T_P$, and $T_4 = 40\,T_P$). It is interesting to compare these results to the deterministic noiseless system. In this case it is simple to estimate error probabilities. Consider the phase space in Figure 1. Since the driving pulse is only applied to the first oscillator, a particle in the upper-right and lower-right quadrants remains there after the pulse is turned off. Moreover, the pulse is strong enough to move a particle from the upper-left to the upper-right quadrant, but it is too weak to force the particle out of the lower-left quadrant (where there is a deep minimum of the potential, as shown in Fig. 2). Therefore, the probability of error for the first oscillator is 1/4. However, the probability of error for the second oscillator depends on the coupling strength. If the coupling is strong, then the output of the first oscillator is capable of driving the second and $p_{e,2} = 1/4$. On the other hand, if the coupling strength is weak, the state of the second oscillator does not change as a consequence of changes in the output of the first and, hence, $p_{e,2} = 1/2$. A small amount of noise is enough to improve memory performance as it allows a particle located in the lower-right quadrant to escape to adjacent wells. Figure 4 shows the positive influence of noise. An antiresonant behavior is readily observed, i.e., the probability of error is optimized for a given noise intensity, a signature of stochastic resonance.

Now we turn to the dynamic behavior of the coupled oscillators. Results shown in Figure 4 indicate that the coupling strength plays a significant role in the dynamics of the memory device: for weak coupling strengths the minimum p_e increases with time (i.e., memory performance degrades), whereas it remains approximately constant for a strong coupling strength. This is a desirable feature for the practical application of this device, as it points to a system whose performance not only benefits from added noise, but it is also robust in a noisy environment. As expected, in both cases the noise range that yields the minimum p_e decreases with time.

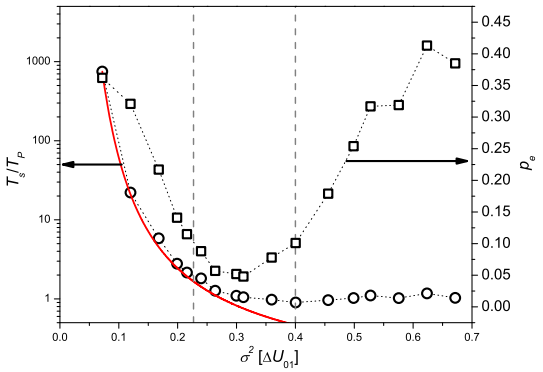

Fig. 5. (Color online) Synchronization time (T_s) and probability of error at T_s as a function of noise intensity. The solid line corresponds to a theoretical approximation to T_s.

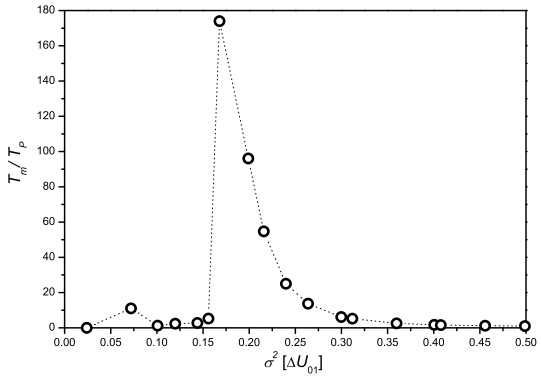

Fig. 6. Persistence time as a function of noise intensity.

3.1 Synchronization and memory persistence

Keeping in mind a practical realization of the coupled double-well system as a one-bit storage device, not only we require information retrieval to be 'asynchronous' in the sense that it is possible to interrogate the system at any time, but also that we obtain a unique value for the memory state when we interrogate any of the two oscillators. We say that the oscillators are 'synchronized' if $p_{e,1}$ and $p_{e,2}$ differ in a small quantity, arbitrarily fixed to 10^{-3}. Results in Figure 3b show the time evolution of the probability of error for three different noise intensities, starting at the time when the external pulse is switched on, until the two oscillators are synchronized. We define the elapsed time between these two events as the synchronization time T_s. By comparing the performance of the two oscillators, we find that, until synchronization is reached, the second oscillator exhibits a worse error rate for all noise levels. This is due to the fact that the external pulse acts exclusively on the first oscillator.

Figure 5 shows the synchronization features (i.e. synchronization time and probability of error at synchronization) as a function of the noise intensity. Interestingly, increasing the noise intensity makes T_s decrease.

The dependence of T_s with noise intensity can be qualitatively explained as follows: suppose that memory retrieval is carried out by instantaneously observing the state of the oscillator, i.e., without computing the average in equation (8). Then, the probability of error can be written in terms of the state probabilities in equation (6) as $p_{e,1}(t) = n_1(t) + n_2(t)$ and $p_{e,2}(t) = n_2(t) + n_3(t)$. Solving equation (6) for a given initial condition, it can be shown that

$$p_{e,1}(t) - p_{e,2}(t) \propto \mathrm{e}^{-2(W_{10}+W_{13})t}. \tag{10}$$

Therefore, the synchronization time is

$$T_s = \frac{\tau}{2(W_{10}+W_{13})}, \tag{11}$$

where τ is a suitably chosen constant. Although we have derived equation (11) assuming instantaneous observations of the oscillators, it is reasonable to expect that the equation is still approximately valid when the average in equation (8) is computed for $T_s > T_P$. The solid line in Figure 5 corresponds to equation (11), with W_{10} and W_{13} computed as described in equation (7) and τ calculated by fitting T_s for the smallest noise intensity. As it can be observed, there is a good agreement between equation (11) and the simulation results for $T_s > T_P$.

From Figure 5, we observe that there is a range of noise intensities, enclosed by vertical dashed lines, for which both p_e is small and T_s is close to its minimum, i.e, the device performs well and any of the two oscillators can be interrogated, at any time, in order to retrieve the memory state.

Finally, we propose the following criterion as a way to characterize the persistence time of the memory, (T_m): we take (T_m) as the time elapsed until the first oscillator reaches a probability of error equal to that of the noiseless case, i.e, from that point on, noise no longer helps improve device performance. This definition allows us to specify a 'refresh' time scale, in a similar fashion as in common DRAM devices (see, e.g., [35]). Observe that, from Figure 6 where T_m is shown as a function of noise intensity and for a weak coupling strength, T_m presents a stochastic resonance characteristic. The explanation of this behavior lies in the fact that, for an optimal noise level, the system easily moves to the upper-right equilibrium state, but hardly ever leaves it. Indeed, by pairing two oscillators the memory device turns out to be more stable, i.e., it can be easily shown that the persistence time of the device is much longer than the Kramer's escape time of a single oscillator. Note, also, that there is an optimal noise range for which *the persistence time is maximized, both oscillators are synchronized, and the probability of error is minimal.*

4 Experimental results

In this section we present experimental results corresponding to a ring of two Schmitt triggers. We use STs as 'discrete' models of the bistable potentials in previous sections. A single pulse, representing the '1' state that is to be stored, is fed into the first ST with a supra-threshold amplitude of +5 V and duration $T_P = 1$ ms. ST thresholds

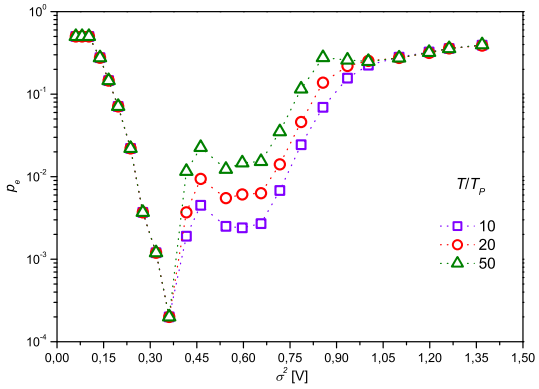

Fig. 7. (Color online) Experimental results for a loop of two STs: memory performance as a function of the noise intensity and time.

are set to +3 V and −1 V, respectively. The output of the first ST, set to sub-threshold values of +2 V and 0 V respectively, is used to drive the second ST. Then, the output of the second ST is fed back into the first ST and we allow for a delay of $t = 98T_P$ before refreshing the memory by again applying the driving pulse. In the experimental setup, noise is generated by low-pass filtering of a pseudo-random bit sequence (PRBS) generator working at a rate of 250 kHz [36]. Since the filter cutoff 3-dB bandwidth is chosen greater than 10 KHz, the noise spectral density is flat over the studied range.

During the time when the system is not driven, we interrogate the second ST at intervals of T_P. As discussed in previous sections, the detector averages the received amplitude over a fraction of T_P and compares it to a fixed threshold, in order to make a decision between a '1' and a '0' states. Finally, we repeat this procedure 10000 times, alternating the initial state of the second ST, and compute the probability of error by counting the number of times a '0' state was detected.

Figure 7 shows the estimated probability of error as a function of noise intensity and elapsed time. As it can be observed, p_e behaves in a similar manner as in Figure 4d. For instance, $p_e = 1/2$ for low noise intensities because the sub-threshold output of the first ST is not strong enough to drive the second ST. It can also be observed that there is a range of noise that minimizes the probability of error, a signature of stochastic resonance which is also present in the results in Figure 4. Also, close to the optimum noise intensity, device performance does not degrade with time. In summary, experimental results obtained with discrete bistable potentials built around Schmitt triggers confirm the existence of an optimal noise intensity for the probability of error of the proposed memory device, paving the way for a practical implementation.

5 Conclusions

In this work, we studied the dynamical behavior of a system comprised of two bistable oscillators in a loop configuration. In particular, we showed that such a system is capable of storing a single bit of information in a noisy environment. Furthermore, by calculating the probability of error upon retrieval of the stored bit, we showed that performance in the presence of noise exceeds that of the deterministic noiseless system, a signature of stochastic resonance.

The proposed device can be regarded as asynchronous, in the sense that stored information can be retrieved at any time. Moreover, after a certain 'synchronization' time, the probability of erroneous retrieval does not depend on which oscillator is being interrogated. Interestingly, we found that there is a range of noise intensities which both minimizes the probability of error and the synchronization time.

System performance was also characterized by the memory persistence time, which we defined as the time elapsed until the probability of error equals that of the noiseless case. We found that this persistence time is maximized for the same noise range that minimizes the probability of error and ensures synchronization.

Finally, we built a model of the proposed device by means of a loop of two Schmitt triggers, acting as 'discrete' analogues of the bistable oscillators. We were able to show experimentally that this system is capable of storing a single bit and does so more efficiently in the presence of noise.

In summary, we believe that the proposed device may serve as a building block for future computing systems which, due to the increasing scale of integration, will have to deal with smaller noise margins.

References

1. P. Korkmaz, B.E.S. Akgul, K.V. Palem, IEEE Trans. Circuits Syst. I: Regular Papers **55**, 2249 (2008)
2. L.B. Kish, Phys. Lett. A **305**, 144 (2002)
3. L.B. Kish, IEE Proc.-Circuits Devices Syst. **151**, 190 (2004)
4. K.V. Palem, IEEE Trans. Comput. **54**, 1123 (2005)
5. R. Bahar, J. Mundy, J. Chen, A probabilistic-based design methodology for nanoscale computation, in *ICCAD '03: Proceedings of the 2003 IEEE/ACM international conference on Computer-aided design* (IEEE Computer Society, Washington, DC, USA, 2003), pp. 480–486
6. L.B. Kish, Phys. Lett. A **373**, 911 (2009)
7. K. Murali, S. Sinha, W.L. Ditto, A.R. Bulsara, Phys. Rev. Lett. **102**, 104101 (2009)
8. K. Murali, I. Rajamohamed, S. Sinha, W.L. Ditto, A.R. Bulsara, Appl. Phys. Lett. **95**, 194102 (2009)
9. S. Sinha, J.M. Cruz, T. Buhse, P. Parmananda, Europhys. Lett. **86**, 60003 (2009)
10. R. Benzi, A. Sutera, A. Vulpiani, J. Phys. A **14**, L453 (1981)
11. B. McNamara, K. Wiesenfeld, Phys. Rev. A **39**, 4854 (1989)
12. L. Gammaitoni, P. Hänggi, P. Jung, F. Marchesoni, Rev. Mod. Phys. **70**, 223 (1998)
13. K. Wiesenfeld, F. Moss, Nature **373**, 33 (1995)
14. Y. Sakumura, K. Aihara, Neural Process. Lett. **16**, 235 (2002)

15. D. Rousseau, F. Chapeau-Blondeau, Neural Process. Lett. **20**, 71 (2004)
16. F. Chapeau-Blondeau, Electron. Lett. **35**, 1055 (1999)
17. F. Chapeau-Blondeau, J. Rojas-Varela, Int. J. Bifur. Chaos **10**, 1951 (2000)
18. J.F. Lindner, S. Chandramouli, A.R. Bulsara, M. Löcher, W.L. Ditto, Phys. Rev. Lett. **81**, 5048 (1998)
19. M. Löcher, D. Cigna, E.R. Hunt, Phys. Rev. Lett. **80**, 5212 (1998)
20. J. García-Ojalvo, A.M. Lacasta, F. Sagués, J.M. Sancho, Europhys. Lett. **50**, 427 (2000)
21. G.A. Patterson, A.F. Goya, P.I. Fierens, S.A. Ibáñez, D.F. Grosz, Physica A **389**, 1965 (2010)
22. S.A. Ibáñez, P.I. Fierens, R.P.J. Perazzo, D.F. Grosz, Fluc. Noise Lett. **8**, L315 (2008)
23. S.A. Ibáñez, P.I. Fierens, R.P.J. Perazzo, D.F. Grosz, Physica D **238**, 2138 (2009)
24. M.F. Carusela, R.P.J. Perazzo, L. Romanelli, Phys. Rev. E **64**, 031101 (2001)
25. M.F. Carusela, R.P.J. Perazzo, L. Romanelli, Physica D 177 (2002)
26. M.F. Carusela, L. Romanelli, Adv. Complex Syst. (ACS) **11**, 55 (2008)
27. S. Fauve, F. Heslot, Phys. Lett. A **97**, 5 (1983)
28. M.F. Carusela, J. Codnia, L. Romanelli, Physica A **330**, 415 (2003)
29. A. Neiman, Phys. Rev. E **49**, 3484 (1994)
30. J.A. Acebrón, A.R. Bulsara, M.E. Inchiosa, W.J. Rappel, Europhys. Lett. **56**, 354 (2001)
31. J.A. Acebrón, W.J. Rappel, A.R. Bulsara, Phys. Rev. E **67**, 016210 (2003)
32. H.A. Kramers, Physica **7**, 284 (1940)
33. C.W. Gardiner, *Handbook of Stochastic Methods: for Physics, Chemistry and the Natural Sciences*, 3rd edn. (Springer Series in Synergetics, Springer, 2004)
34. T.C. Gard, *Introduction to Stochastic Differential Equations* (Marcel Dekker, 1988)
35. D.T. Wang, Ph.D. thesis, University of Maryland, 2005
36. P. Horowitz, W. Hill, *The Art of Electronics* (Cambridge University Press, New York, NY, USA, 1989)